

CrossMark  
click for updatesCite this: *Mater. Horiz.*, 2015, 2, 245Received 31st October 2014  
Accepted 27th November 2014

DOI: 10.1039/c4mh00210e

rsc.li/materials-horizons

# An ultrastable porous metal–organic framework luminescent switch towards aromatic compounds†

Fei-Yan Yi,<sup>a</sup> Ying Wang,<sup>a</sup> Jian-Ping Li,<sup>a</sup> Dai Wu,<sup>a</sup> Ya-Qian Lan<sup>\*b</sup> and Zhong-Ming Sun<sup>\*a</sup>

In this work, a highly stable MOF luminescent switch  $\{Cd_3(L)(bipy)_2 \cdot 4DMA\}_n$  (**1**) has been successfully constructed, which exhibits clear fluorescence enhancement and “turn-off” quenching responses for benzene and nitrobenzene vapors, respectively, with high selectivity and sensitivity, as well as being fully reusable. Remarkably, the porous MOF (**1**) remains intact in aqueous solution over an extensive pH range of 2–13. This MOF sensor realizes fast detection for benzene vapor with a response time of less than one minute and ~8-fold fluorescence enhancement. Furthermore, it as a porous multifunctional MOF also shows fully reversible adsorption behaviour for benzene vapor at room temperature. Thus the MOF material will be a promising luminescent sensor and adsorbent material for benzene vapor with important practical applications from environmental and health points of view.

## Introduction

Rapid detection and reduction of volatile organic compounds (VOCs) are very important subjects of widespread societal concern related to environmental and health issues.<sup>1</sup> The release of VOCs as main sources of atmospheric pollution such as aromatic species (benzene, nitroaromatic explosives, *etc.*) also poses various threats to homeland security. So it is a critical and significant task to selectively recognize these harmful small molecules, and subsequently to be efficient enough to eliminate them. Particularly, benzene as a colourless and highly volatile

### Conceptual insights

Fluorescence chemosensors as an expedient detection technique have been widely used for the detection of common volatile organic compounds (VOCs). They have many advantages over other sophisticated electrochemical devices, such as high signal output, simple detection, low expense, and reliability. Metal-organic framework (MOF) materials are promising luminescent sensors as their structures and functions are systematically and predictably designable and readily modulated. The reported MOF sensors have also verified their effectiveness, but most of those explored thus far show only a single “turn-off” or “turn-on” luminescence response for solvent solution. These are not efficient enough for detecting trace solvent vapors. In this paper we successfully synthesized an ultrastable MOF sensor, which realizes excellent ‘on-off’ switch-functions for the probing of benzene and nitrobenzene vapor. We investigate its various parameters to assess the practicality of the sensor, such as selectivity, sensitivity, response rate, repeatability and stability. This MOF-based luminescent switch opens up a new sensor platform with unprecedented practical applications.

liquid can lead to the reduction of leukocytes, and even leukaemia,<sup>2</sup> so the determination of indoor benzene vapor is extremely important. Till now, besides sophisticated and expensive electrochemical devices,<sup>3</sup> some metal coordination and other reported systems, such as organic–inorganic hybrids, as expedient luminescent sensing methods have been used in the detection of VOCs,<sup>4</sup> but it has not been reported that a practical sensory material can effectively detect benzene vapor with high sensitivity and fast response. Metal–organic frameworks (MOFs),<sup>5</sup> also known as porous coordination polymers, are attractive for these purposes because (1) their structural and chemical tunability can afford good selectivity through pore sieving functions with different pore sizes or host framework–guest interactions; (2) MOFs with high internal surface areas can concentrate analytes to high density, thereby decreasing detection limits and exhibiting high sensitivity; (3) another striking feature of porous MOFs is their ability to remove polluting guest small molecules as adsorbents. Therefore, MOFs as fluorescent sensing materials are of considerable interest and have been widely explored by researchers.<sup>6–8</sup>

<sup>a</sup>State Key Laboratory of Rare Earth Resource Utilization, Changchun Institute of Applied Chemistry, Chinese Academy of Sciences, 5625 Renmin Street, Changchun, Jilin 130022, P. R. China. E-mail: szm@ciac.ac.cn; Web: <http://zhongmingsun.weebly.com>

<sup>b</sup>School of Chemistry and Materials Science, Nanjing Normal University, Nanjing 210023, P. R. China. E-mail: yqlan@njnu.edu.cn

† Electronic supplementary information (ESI) available: Materials and methods, crystal data, structural information, PXRD, FTIR, TGA, fluorescence measurements, UV-Vis and additional figures. CCDC 1017377. For ESI and crystallographic data in CIF or other electronic format see DOI: 10.1039/c4mh00210e

Furthermore, MOF-based fluorescent sensors exhibit many advantages such as high signal output, simple detection, low cost, and good reliability, which are of great significance for practical use of the sensors. Although there are a number of reports on MOF sensors or guest-dependent luminescence for common small molecular solvents (for example, Li and Chen *et al.*<sup>9</sup> have reported “turn-off” luminescence sensors for nitrobenzene based on a quenching mechanism), fluorescent sensing of trace solvent vapors is still challenging due to their low vapor pressures at room temperature, so the luminescence detection in the vapor phase is much more difficult than in the liquid form.<sup>10</sup> Fluorescence enhancement is more attractive and rare; a MOF-based luminescent switch showing clearly two functions of fluorescence enhancement and quenching effects has not been explored until now.<sup>9f</sup> So the exploitation of novel and efficient MOF sensory on-off materials for the detection of vaporized analytes is progressing with an extraordinary effort. Herein, we report a porous Cd-MOF as a luminescent switch exhibiting significant fluorescence enhancement for benzene vapor and a turn-off quenching effect for nitrobenzene vapor. This MOF material features very fast response rate, full reusability, and high sensitivity. Notably, it exhibits excellent water stability and chemical stability. Furthermore, it shows fully reversible adsorption behavior for benzene vapor at room temperature. To the best of our knowledge, no available literature thus far has investigated a MOF sensory material showing high selectivity and sensitivity for trace benzene vapor based on significant fluorescence enhancement.<sup>9f,11</sup>

## Experimental

### Synthesis of $\{\text{Cd}_3(\text{L})(\text{bipy})_2 \cdot 4\text{DMA}\}_n$ (**1**)

A mixture of  $\text{Cd}(\text{NO}_3)_2 \cdot 4\text{H}_2\text{O}$  (0.12 mmol, 37.0 mg),  $\text{H}_6\text{L}$  (0.04 mmol, 39.0 mg) and bipy (0.12 mmol, 18.7 mg) in mixed *N,N'*-dimethylacetamide (DMA, 6 mL)/distilled water ( $\text{H}_2\text{O}$ , 1 mL) solvents was sealed in a 20 mL pressure-resistant Teflon-lined stainless steel vessel, and heated in an oven to 100 °C for 3 days, and then slowly cooled to room temperature. The colorless rodlike crystals of **1** were obtained in a yield of 66.1 mg (84% based on  $\text{Cd}^{\text{II}}$ ), and washed with distilled water ( $\text{H}_2\text{O}$ ). The purity was confirmed by PXRD (see the ESI<sup>†</sup>). Anal. Calcd (%) for **1**  $\text{C}_{88}\text{H}_{92}\text{Cd}_3\text{N}_8\text{O}_{23}$  ( $M_r = 1966.9$ ): C, 53.74; H, 4.71; N, 5.70. Found: C, 53.91; H, 4.84; N, 5.66. IR peaks ( $\text{cm}^{-1}$ ) for **1**: 3432 (w), 3097 (w), 2942 (w), 2879 (w), 1671 (m), 1604 (s), 1512 (vs), 1415 (m), 1384 (m), 1332 (w), 1296 (s), 1250 (vs), 1162 (m), 1106 (m), 1049 (m), 998 (m), 957 (m), 905 (m), 843 (w), 813 (m), 766 (w), 735 (w), 658 (m).

### Fluorescence measurements

The luminescent properties of Cd-MOF (**1**) were examined in the solid state, in organic solvent suspensions and vapors at room temperature. The photoluminescence (PL) excitation and emission spectra were recorded on a Hitachi F-7000 spectrophotometer equipped with a 150 W xenon lamp as the excitation source. Prior to the measurements, some preparatory work was done. The as-synthesized sample of **1** was immersed into

anhydrous methanol for 3 days, methanol was refreshed three times during the exchange. Then similar immersion was utilized to treat the sample with dichloromethane to remove methanol molecules. After the removal of dichloromethane by centrifuging, the wet sample was dried under vacuum at 80 °C for 15 h to yield activated **1** (denoted as **1a**). Solid samples of activated **1a** were ground into powder and used for vapor sensing experiments.

**1a** (30 mg) was placed into a glass tube (5 mL), then put under different solvent vapors for 24 h, including benzene, benzene- $\text{d}_6$  ( $\text{C}_6\text{D}_6$ ), toluene, 1,2-dichlorobenzene, 4-chlorotoluene, bromobenzene, nitrobenzene, nitromethane, methanol, ethanol,  $\text{CH}_2\text{Cl}_2$ ,  $\text{CCl}_4$ , 2-propanol, phenylmethanol and  $\text{H}_2\text{O}$ . Subsequently the sample tube was taken out and quickly sealed, then the emission spectra were recorded.

The **1a** sample used as *in situ* time-dependent photoluminescence sensor for solvent vapors was prepared as follows. A ground sample of **1a** (100 mg) was pressed into a firm sheet, which was attached to a quartz slide and placed into a cuvette about 1.2 cm from the bottom. The cuvette containing the sensor slide was positioned on the solid sample holder of a Hitachi F-7000 spectrophotometer. The solid state emission spectra of firm sheet sample were recorded as an initial standard, then  $\sim 120 \mu\text{L}$  benzene (or benzene- $\text{d}_6$ , nitrobenzene) solution was carefully added into the cuvette. The volume of cuvette used was  $2 \text{ cm}^3$  with a length and width of 1 cm and a height of 2 cm. So the concentration of the targeted solvent vapor in the cuvette was about  $52.6 \text{ mg cm}^{-3}$  ( $0.67 \text{ mmol cm}^{-3}$ ).

## Results and discussion

The Cd-MOF sensory material was synthesized by mixing a hexacarboxylate ligand  $\text{H}_6\text{L}$  (hexa[4-(carboxyphenyl)oxamethyl]-3-oxapentane acid) (Scheme S1<sup>†</sup>) with  $\text{Cd}(\text{NO}_3)_2 \cdot 4\text{H}_2\text{O}$  and coligand bipy (bipy = 2,2'-bipyridine) *via* a solvothermal method in mixed solvent *N,N'*-dimethylacetamide (DMA)/distilled water ( $\text{H}_2\text{O}$ ) at 100 °C for 3 days. It was formulated as  $\{\text{Cd}_3(\text{L})(\text{bipy})_2 \cdot 4\text{DMA}\}_n$  (**1**) based on elemental analysis, single-crystal X-ray diffraction study, thermogravimetric analysis (TGA), and powder XRD analysis. Compared with the previously reported ligands,  $\text{H}_6\text{L}$  is flexible and can be restricted to different functional conformations during the formation of MOFs, leading to different fluorescent responses. The constructed flexible framework is very sensitive to external stimuli: it can shrink or expand (breathing effect) for the removal or addition of guest species, making it effective as a fluorescent sensor.

Single-crystal X-ray diffraction analysis reveals that **1** crystallizes in a monoclinic  $C2/c$  space group (Table S1<sup>†</sup>).<sup>‡</sup> In **1**, two Cd(1) situated at the two ends and one Cd(2) at the center form a trinuclear secondary building unit (SBU) ( $\text{Cd}_3^{\text{II}}$ ) (Fig. 1a). In this SBU, Cd(1) is sevenfold-coordinated by two N atoms of one 2,2'-bipy ligand and five carboxylate oxygen atoms from three  $\text{L}^{6-}$  ligands in a distorted  $\{\text{CdN}_2\text{O}_5\}$  pentagonal bipyramid geometry. The Cd(2) ion lies at an inversion centre and thus has 1/2 occupancy, adopting the typical  $\{\text{CdO}_6\}$  octahedral coordination mode with six carboxylate oxygen atoms of *anti-anti*

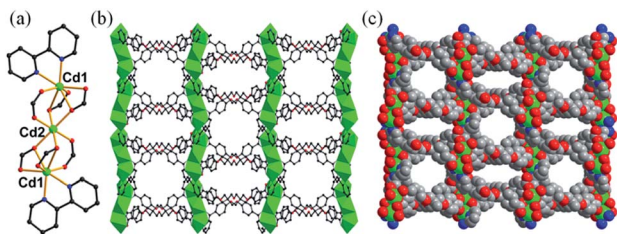


Fig. 1 (a) Cd<sub>3</sub> SBU. (b) View of the 3D porous framework along the *c*-axis. (c) The face-filling representation of **1**. Color mode: Cd, green; C, grey; N, blue; O, red.

coordination conformations from four L<sup>6-</sup> ligands (Fig. S1†). The bond lengths of Cd–O and Cd–N in the range 2.166(7)–2.587(6) Å and 2.330(9)–2.392(11) Å, respectively, are comparable to reported values.<sup>12</sup> Each unique L<sup>6-</sup> ligand with six carboxylate arms links ten Cd atoms by four  $\mu_2$ - $\eta^1, \eta^2$  carboxylate groups and two  $\mu_2$ - $\eta^1, \eta^1$  ones. Each SBU is connected to four adjacent units *via* four L<sup>6-</sup> ligands to further form a 2D double layer (Fig. S2†), which stack together to give the overall 3D structure with one-dimensional (1D) open channels having approximate sizes of 16.3 × 11.7 Å<sup>2</sup> and 11.5 × 10.9 Å<sup>2</sup> along the *c*-axis and 5.1 × 8.5 Å<sup>2</sup> along the *b*-axis (measured between opposite atoms without taking van der Waals radii of the atoms into account) (Fig. 1b and c). The free DMA guest molecules reside in the channels (Fig. S3†). The overall structure can be simplified into a (4,4)-connected uninodal *sql* double layer (Fig. S4†) analyzed by the freely available computer program TOPOS.<sup>13</sup> The solvent-accessible volume was calculated to be 43.3% by PLATON.<sup>14</sup>

The TGA result of activated **1** (see the ESI and Fig. S5†) indicates **1** may completely release its free solvent molecules to form guest-free **1** (referred to as **1a** hereafter). The resulting **1a** is thermally stable up to 265 °C. Adsorption and desorption

isotherms of N<sub>2</sub> (Fig. 2a) for **1a** exhibit a single step type I curve with Brunauer–Emmett–Teller (BET) and Langmuir surface areas of 475.0 and 698.6 m<sup>2</sup> g<sup>-1</sup>, respectively, as well as a total pore volume of 0.25 cm<sup>3</sup> g<sup>-1</sup>. The pore size distribution (Fig. S6†) is around 8.6–9.3 Å, matching well with the crystal structure model. The adsorption isotherms of H<sub>2</sub> at 77 and 87 K, and of CO<sub>2</sub> at 273 and 298 K, were also measured up to 1 atm (Fig. 2a). They show smooth type-I isotherms with uptakes of 129.8 cm<sup>3</sup> g<sup>-1</sup> at 77 K and 96.0 cm<sup>3</sup> g<sup>-1</sup> at 87 K for H<sub>2</sub>, 50.9 cm<sup>3</sup> g<sup>-1</sup> at 273 K and 32.0 cm<sup>3</sup> g<sup>-1</sup> at 298 K for CO<sub>2</sub>. All of the above results demonstrate the robustness and the permanent microporous nature of **1a**. More interesting is that **1** can be regenerated by soaking **1a** in DMA. Such release and capture for solvent molecules are desirable characteristics, which prompted us to examine its ability as a potential sensory material and adsorbent for solvents. In addition, **1a** is insoluble in water and common organic solvents, and it can still remain intact in the air for 3 months and in aqueous solution for 7 days (Fig. 2c). Each ground sample of **1a** (30 mg) was immersed into aqueous solutions with different pH values from 1 to 13 for 24 h, then separated by simple centrifugation, washed three times with water (3 mL), then dried at 50 °C for 12 h. Their PXRD results (Fig. 2d) reveal that the characteristic peaks maintain nearly the same positions as those of as-synthesized **1a** over a wide pH range from 2 to 13, suggesting that **1a** is chemically stable with strong acid and base resistance, which is prerequisite for many important industrial applications. Meanwhile, the PXRD patterns and FTIR spectra also further illustrate its good water/solvent stability after solvent treatment (Fig. S7–S10†). Such high water stability and chemical stability demonstrate that **1a** is ultrastable. Adding its thermal stability and porous characteristics lays a firm foundation for the further practical study of this material in chemical sensing applications.

As shown in Fig. S11,† **1a** exhibits a broad luminescence emission centered at ~427 nm upon excitation at 324 nm. Compared to those of the neutral ligands H<sub>6</sub>L (three bands: 382, 401 and 423 nm) and bipy (two shoulder peaks: 392 and 411 nm), the emission band of **1a** covers the whole range of H<sub>6</sub>L and bipy ligands, concomitant with a red shift of ≈16–26 nm, hence it can be assigned to ligand-to-ligand charge transition (LLCT), admixing with metal-to-ligand transition (MLCT) for such Cd<sup>2+</sup> coordination complexes.<sup>6b,k,l</sup> The ground powder of **1a** was put under water and organic solvent vapors (such as methanol, ethanol, CH<sub>2</sub>Cl<sub>2</sub>, CCl<sub>4</sub>, 2-propanol, phenylmethanol, benzene, toluene, bromobenzene, 1,2-dichlorobenzene, 4-chlorotoluene, nitrobenzene, 2,4-dinitrotoluene, and nitromethane) for 24 h (Fig. S12†). Notably, **1a** shows significantly different luminescence responses (Fig. 3 and S13†) toward the vaporized analytes: an ~8-fold fluorescence enhancement and a strong ‘turn-off’ fluorescence quenching effect occurred after exposure to benzene and nitro-explosives vapors, respectively. The results of the enhancing or quenching levels are in accordance with the ones in liquid media (Fig. S14†). More dramatically, **1a** after exposure to benzene (**1a**/benzene) exhibits a hypsochromic shift of ~67 nm ( $\lambda_{\max} = 381$  nm, violet color) compared with **1a**/nitro-aromatic explosives ( $\lambda_{\max} = 448$  nm, blue color; Fig. S13c†). Such a luminescence enhancement effect, where the presence

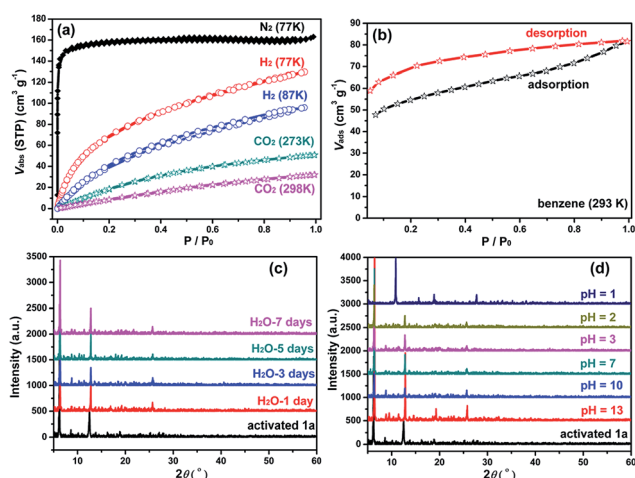


Fig. 2 (a) Gas adsorption and desorption isotherm of **1a** for N<sub>2</sub> at 77 K (black), H<sub>2</sub> at 77 K (red) and 87 K (blue), CO<sub>2</sub> at 273 K (green) and 298 K (pink). (b) Vapor sorption isotherms for benzene at 293 K. (c) PXRD patterns of **1a** after immersed in H<sub>2</sub>O for different times: one day, three days, five days, and seven days. (d) PXRD patterns of **1a** in different pH solutions for 1 day.

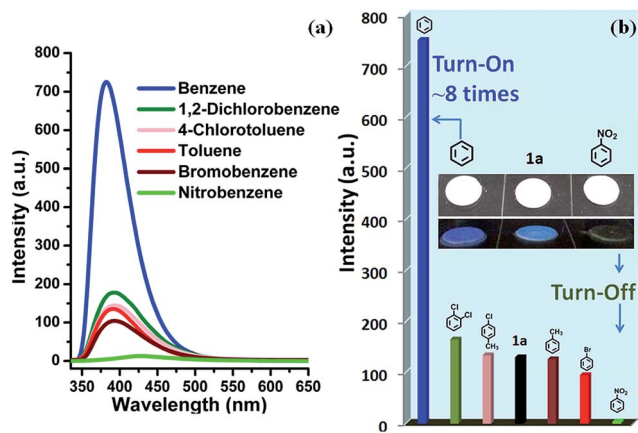


Fig. 3 (a) The luminescence spectra of **1a** after incubation for 24 h under various solvent vapors when excited at 314 nm. (b) The related luminescence intensity ( $\lambda_{\text{em}} = 381$  nm). The inset shows a comparison diagram of fluorescence for **1a**, **1a**/benzene and **1a**/nitrobenzene in UV light.

of the analyte triggers an increase in the luminescence intensity, is rare; in particular, high selectivity for benzene vapor with a colour shift in the emission wavelength is much rarer and practical. Interestingly, when benzene- $d_6$  ( $C_6D_6$ ) was employed as the target vapor, a clearly different fluorescent intensity from **1a**/benzene was observed (Fig. S13d<sup>†</sup>), and an  $\sim 4$ -times fluorescence enhancement was obtained. To further understand the energy levels of **1a** in different solvents environment and host-guest interactions, a theoretical calculation using the Gaussian 09 package was employed based on an idealized non-periodic cluster model constructed according to the experimental data and the computational details are depicted in the ESI.<sup>†</sup> The calculation results are shown in Fig. 4, and indicate that the electron density of the highest occupied molecular orbital (HOMO) is dominated by  $p$ -orbitals of the carboxylate ligand, and the lowest unoccupied molecular orbital (LUMO) is mainly distributed on the N and C atoms in the bipy aromatic ligand. So the energy transfer from the carboxylate ligand to bipy ligand contributes directly to the luminescence of **1a**. The

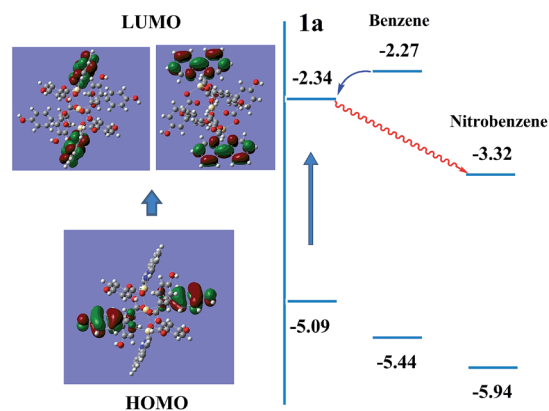


Fig. 4 Schematic drawings of the electronic structures of **1a** in benzene and nitrobenzene environments.

corresponding calculated energy gap is *ca.* 2.75 eV (*ca.* 450 nm), which is far from the experimental fluorescence data (427 nm). That may be caused by the computational method or the selected ideal structural model of (1) a non-periodic basic trinuclear cluster, and (2) deleting all free solvent molecules, because the crystal data is actually periodic and it is difficult to completely remove all free solvent molecules in its channels although some preparatory work has been done. Such ligand-based emission in MOFs is more desirable, since the bandgaps of these materials can be altered by changing the degree of conjugation in the ligand, affecting the intensity and position of emission.<sup>15</sup> In host-guest chemistry, exchanged solvent molecules can diffuse into the channels, leading to the different fluorescent responses by analyte-ligand interactions.

For **1a**/benzene, the calculated energy gap increases from 2.75 eV to 3.17 eV, and the difference (0.42 eV) relative to **1a** is very close to the observed blue-shift in the experiment of the luminescence (0.49 eV). Its LUMO is at a high-lying  $\pi^*$  anti-bonding state with higher energy, so energy transfer from benzene to the LUMO of compound **1** occurs and leads to a fluorescence enhancement upon excitation. The significant shifting of emission  $\lambda_{\text{max}}$  and fluorescence enhancement could be ascribed to the  $\pi \cdots \pi$  stacking interaction between MOF host and benzene molecules, so that the energy levels of the ground state and excited state were changed (Fig. 4). In contrast, the excited electrons are transferred from the LUMO of **1** to nitrobenzene, thereby leading to a quenching effect for **1a**/nitrobenzene. This mechanism is consistent with one previously proposed by other groups and us.<sup>9f,16</sup> The UV-Vis adsorption spectra (Fig. S15<sup>†</sup>) of **1**, ligands ( $H_6L$  and bipy) and solvents (benzene and nitrobenzene) further verify and provide deeper understanding of the luminescent response. It is obvious that the adsorption peaks of **1** and bipy ligand at 220–322 nm almost cover the entire range of the absorption of solvents. Upon illumination, there is competition for excitation energy between the absorption of nitrobenzene and **1** because of the presence of the electron-withdrawing  $-NO_2$  group, whereas benzene molecules may have a similar excited energy level to **1a**, which has been confirmed by experimental results. As shown in Fig. S16,<sup>†</sup> the fluorescent spectrum of pure benzene solution exhibits a main sharp emission maxima at *ca.* 328 nm and one very weak sloping band at  $\sim 390$  nm under normal 286 nm excitation. When under excitation at 314 nm, which is the excitation condition of **1a**, benzene molecules can emit very weakly at  $\lambda_{\text{max}} = 386$  nm. Combined with the UV-Vis absorption data, it is most likely to lead to energy transfer from benzene to **1a** or bipy ligands under excitation, which results in the increase of the luminescent intensity.<sup>11b</sup>

In order to test the sensitivity and response rate of **1a** as a vapor sensor, an *in situ* solid-state luminescent sensor setup was designed and used (Fig. 5). The time-dependent enhancing and quenching efficiency shows that the response rate of **1a** for benzene vapor is 56 s, and it exhibits  $\sim 8$  fold fluorescence enhancement in 2–3 min (Fig. S17<sup>†</sup>); for benzene- $d_6$  vapor it is 30 s and reaches the maximum ( $\sim 4$  times fluorescent intensity) in 2 min (Fig. S18<sup>†</sup>); and the fluorescence quenching for nitrobenzene reaches a maximum in 1 min with a quenching

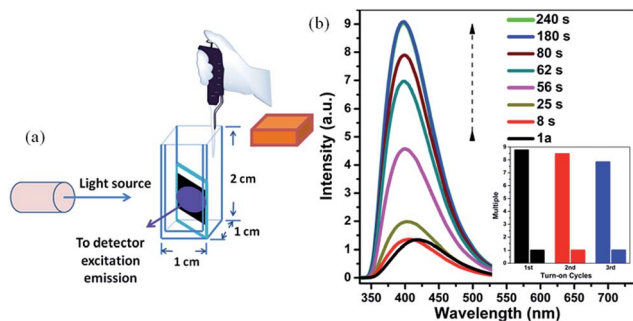


Fig. 5 (a) *In situ* solid-state luminescent sensor setup. (b) Emission spectra of **1a** upon exposure to benzene vapor at various time intervals at room temperature. The inset shows three consecutive enhancement and regeneration cycles.

percentage of more than 90% (Fig. S19<sup>†</sup>). Such rapid, sensitive response to benzene vapor is still challenging. Repeatability for a sensory material is a very important parameter to assess the sensor practicability. After detection of benzene and nitrobenzene, samples of **1a**/benzene and **1a**/nitrobenzene can be recovered by simply heating at 80 °C under vacuum for 3 h, which can be evidenced by the PXRD patterns (Fig. S8<sup>†</sup>), FTIR spectra (Fig. S10<sup>†</sup>) and TGA curves (Fig. S20<sup>†</sup>). For **1a**/benzene, its PXRD characteristic peaks match well with the ones of as-synthesized **1a**, just the relative intensity shows a slight change (Fig. S8c<sup>†</sup>), which may be attributed to the benzene molecules filling into the MOF channels, giving rise to the high electronic density in this direction. The FTIR spectrum of **1a**/benzene exhibits an obviously increasing infrared absorption peak around 676 cm<sup>-1</sup> that belongs to the frame vibration absorption of benzene rings (Fig. S10k and l<sup>†</sup>) in the channels of **1a**. The PXRD of **1a**/nitrobenzene undergoes a small shift of ~0.23° toward low angle and shows a few new peaks compared with **1a**. So the interlayer distance along the (200) direction increases by 1.1 Å according to Bragg's equation. These changes evidence the structural change of **1a**, caused by a large number of nitrobenzene molecules inserting in the channels of **1a** as well as the hydrogen bonding and  $\pi \cdots \pi$  interactions between the **1a** host and nitrobenzene molecules. The IR spectrum for **1a**/nitrobenzene further verifies (1) the presence of nitrobenzene molecules, where -NO<sub>2</sub> characteristic  $\nu_s$  and  $\nu_{as}$  stretching vibrations (~1519 cm<sup>-1</sup> and ~1343 cm<sup>-1</sup>) as labelled can be apparently observed (Fig. S10m and n<sup>†</sup>); (2) the stretches are associated with the inserted nitrobenzene molecules; (3) the framework of **1a**/nitrobenzene keeps constant as **1a**. The PXRD and IR results for **1a** after heating treatment from **1a**/benzene are in accordance with the ones of **1a**-as-synthesized. The PXRD pattern for **1a** regenerated from **1a**/nitrobenzene also returns to be consistent with the initial one of **1a**-as-synthesized. The -NO<sub>2</sub> characteristic peaks decrease clearly in its IR spectrum. The changes during the adsorption and desorption processes suggest the "breathing effect" occurs in the flexible framework. Then a recovered **1a** sample was reused in the next cycle. The results are presented in Fig. 4b and S17–S19.<sup>†</sup> It was observed that the response rate and sensitivity after three cycles were

mainly maintained, and its PXRD patterns after treatment with benzene and nitrobenzene match well with the simulated pattern generated from the result of single-crystal diffraction data and as-synthesized product (Fig. S8<sup>†</sup>), confirming its good stability and reusability. The foregoing two aspects of rapid response and repeatability are of great significance for practical use of the sensor. One interesting feature can be easily observed during the process of *in situ* luminescent test: the emission wavelength of **1a**/benzene is gradually blue-shifted as time increases. To deeply understand the influence of retention time for **1a** in benzene vapor on its luminescence, a series of detailed studies were carried out, where the PL spectra of **1a** in excess benzene vapor for different time intervals were recorded and are shown in Fig. S21.<sup>†</sup> These results show that the blue-shift is very rapid at the beginning and is complete after about 6 h, which is exactly identical with the foregoing results in Fig. 3 and 5.

As depicted in the experimental section, all *in situ* fluorescent tests were observed based on a concentration of 52.6 mg cm<sup>-3</sup> for benzene vapor (~120  $\mu$ L). The fluorescent intensity change is similar to that with higher benzene concentration as shown in Fig. 3, where the sample was placed in excess benzene vapor. But it is highly possible that the luminescence enhancement is dependent on the vapor concentration. In order to further clarify the relationship, *in situ* fluorescent experiment was carried out in benzene vapor of a low concentration (8.8 mg cm<sup>-3</sup>; Fig. S22<sup>†</sup>). The observation indicates **1a**/benzene still exhibits a clear enhancement effect, but only ~3-fold luminescence enhancement was observed, which is far less than the ~8-fold enhancement in the vapor concentration of 52.6 mg cm<sup>-3</sup>. This study demonstrates not only that the enhancement is significantly dependent on the concentration of benzene vapor, but also suggests that **1a** may be a potential adsorbent material for benzene.

At the same time, one more important feature is also found that the firm sheet sample used for *in situ* solid-state luminescent testing expanded significantly, even breaking into a lot of small pieces after exposure to benzene vapor, yet not after exposure to nitrobenzene (Fig. S23<sup>†</sup>). This result may be caused by a large amount of adsorption for benzene molecules, so **1a** is a potential MOF adsorbent for benzene vapor. As expected, the total weight of the solid sheet for **1a** after treatment with benzene vapor increases by about 55–80% (repeating three times) of the original weight. The TGA curve of **1a** after immersing in benzene (Fig. S20<sup>†</sup>) shows that a weight loss of ~20% (200 mg g<sup>-1</sup>) from 50 to 250 °C is observed, which is equivalent to approximately 6 molecules per formula unit stably trapped inside the channels. But in fact, the weight loss of benzene adsorbed on the surface began at room temperature, so the amount of benzene molecules trapped by the framework of **1a** is much greater than 20%. Furthermore, the sorption isotherm of benzene (Fig. 2b) by **1a** has been measured and shows a rapid increase in the low-pressure range ( $P/P_0 < 0.1$ ), and then slowly approaches saturation with the amount adsorbed of 81.6 cm<sup>3</sup> g<sup>-1</sup> at  $P/P_0 = 0.99$ , confirming the good adsorption properties of **1a**. The desorption curve shows pronounced hysteresis and incomplete desorption, and does not retrace the adsorption isotherm, which may be attributed to

the pore expansion in **1a** when benzene molecules are adsorbed into the pores. Such a large adsorbed amount of benzene vapor into the channels may be another reason for the luminescence enhancement. But the amount for each of the other solvent vapors is difficult to measure, so the correlation between the adsorbed amounts of vapor molecules and luminescence intensity is still not clear at this moment. Similarly, the sample of **1a** after thermal treatment does not affect the next adsorption. In other words, highly luminescent **1a** will be a potential adsorbent for the removal of benzene molecules based on its high porosity, robust stability and reusability, which is needed as an environmentally friendly and effective method.

## Conclusions

In summary, the porous Cd-MOF material obtained is not only a practical luminescent switch demonstrated experimentally, which represents high selectivity and sensitivity for detecting trace benzene (benzene-d<sub>6</sub>) and nitrobenzene explosives in the vapor phase through a luminescence enhancement and quenching response, respectively, but also an effective adsorbent for benzene vapor with recyclability. Its response time reaches ~56 s for benzene vapor. In addition, its remarkable water and chemical stability as well as reusable characteristics are very important to realize practical use. Further research will be centered on making fluorescent MOF films for more straightforward sensing of vapors, which will be easily manipulated as versatile devices.

## Acknowledgements

This work was supported by NSFC (21171162 and 21201162), SRF for ROCS (State Education Ministry) and Jilin Province Youth Foundation (20130522132JH and 20130522170JH).

## Notes and references

† Crystal data for **1**: C<sub>88</sub>H<sub>92</sub>Cd<sub>3</sub>N<sub>8</sub>O<sub>23</sub>, *M* = 1966.90, monoclinic, space group *C2/c*, *a* = 31.136(9) Å, *b* = 20.048(6) Å, *c* = 15.849(4) Å, *V* = 9390(4) Å<sup>3</sup>, *Z* = 4,  $\mu$  = 0.746 mm<sup>-1</sup>, *D<sub>c</sub>* = 1.391 Mg m<sup>-3</sup>, *F*(000) = 4016, 8371 unique (*R*<sub>int</sub> = 0.0792), *R*<sub>1</sub> = 0.0841, *wR*<sub>2</sub> = 0.2592 (*I* > 2σ(*I*)), GOF = 1.011. Max./min. residual electron density 1.653 and -2.053 e Å<sup>-3</sup>. A total of 10 440 data were measured in the range 1.23 < θ < 25.17°.

- (a) R. E. Hester and R. M. Harrison, *Volatile Organic Compounds in the Atmosphere*, Royal Society of Chemistry, Cambridge, UK, 1995; (b) L. Caprino and G. Tonga, *Environ. Health Perspect.*, 1998, **106**, 115–125; (c) H. Lin, M. Jang and K. S. Suslick, *J. Am. Chem. Soc.*, 2011, **133**, 16786–16789.
- (a) R. Snyder, *J. Toxicol. Environ. Health, Part A*, 2000, **61**, 339–346; (b) C. M. McHale, L. Zhang and M. T. Smith, *Carcinogenesis*, 2012, **33**, 240–252; (c) L. A. Wallace, *Annu. Rev. Energy Environ.*, 2001, **26**, 269–301.
- (a) T. Salthammer and M. Bahadir, *Clean: Soil, Air, Water*, 2009, **37**, 417–435; (b) G. A. Eiceman, J. Gardea-Torresdey, F. Dorman, E. Overton, A. Bhushan and H. P. Dharmasena, *Anal. Chem.*, 2006, **78**, 3985–3996.
- (a) X. Zhang, B. Li, Z.-H. Chen and Z.-N. Chen, *J. Mater. Chem.*, 2012, **22**, 11427–11441; (b) M. A. Rawashdeh-Omary, M. D. Rashdan, S. Dharanipathi, O. Elbjairami, P. Rameshb and H. V. Rasika Dias, *Chem. Commun.*, 2011, **47**, 1160–1162; (c) J. Pang, E. J.-P. Marcotte, C. Seward, R. S. Brown and S. Wang, *Angew. Chem.*, 2001, **113**, 4166–4169; *Angew. Chem., Int. Ed.*, 2001, **40**, 4042–4045; (d) H. Ma, R. Gao, D. Yan, J. Zhao and M. Wei, *J. Mater. Chem. C*, 2013, **1**, 4128–4137; (e) Y. Zhao, H. Lin, M. Chen and D. Yan, *Ind. Eng. Chem. Res.*, 2014, **53**, 3140–3147.
- (a) G. Férey, *Chem. Soc. Rev.*, 2008, **37**, 191–214; (b) O. M. Yaghi, *Nat. Mater.*, 2007, **6**, 92–93; (c) J. An, O. K. Farha, J. T. Hupp, E. Pohl, J. I. Yeh and N. L. Rosi, *Nat. Commun.*, 2012, **3**, 1618; (d) L. J. Murray, M. Dincă and J. R. Long, *Chem. Soc. Rev.*, 2009, **38**, 1294–1314; (e) J. Y. Lee, O. K. Farha, J. Roberts, K. A. Scheidt, S. T. Nguyen and J. T. Hupp, *Chem. Soc. Rev.*, 2009, **38**, 1450–1459; (f) J.-R. Li, J. Sculley and H.-C. Zhou, *Chem. Rev.*, 2012, **112**, 869–932; (g) J.-P. Zhang, Y.-B. Zhang, J.-B. Lin and X.-M. Chen, *Chem. Rev.*, 2012, **112**, 1001–1033; (h) H.-L. Zhou, R.-B. Lin, C.-T. He, Y.-B. Zhang, N. Feng, Q. Wang, F. Deng, J.-P. Zhang and X.-M. Chen, *Nat. Commun.*, 2013, **4**, 3534; (i) H. Furukawa, K. E. Cordova, M. O'Keeffe and O. M. Yaghi, *Science*, 2013, **341**, 974–987; (j) N. W. Ockwig, O. Delgado-Friedrichs, M. O'Keeffe and O. M. Yaghi, *Acc. Chem. Res.*, 2005, **38**, 176–182; (k) S. Horike, D. Umeyama and S. Kitagawa, *Acc. Chem. Res.*, 2013, **46**, 2376–2384.
- (a) L. E. Kreno, K. Leong, O. K. Farha, M. Allendorf, R. P. Van Duyne and J. T. Hupp, *Chem. Rev.*, 2012, **112**, 1105–1125; (b) Y. Cui, Y. Yue, G. Qian and B. Chen, *Chem. Rev.*, 2012, **112**, 1126–1162; (c) B. Chen, Y. Yang, F. Zapata, G. Lin, G. Qian and E. B. Lobkovsky, *Adv. Mater.*, 2007, **19**, 1693–1696; (d) B. Chen, L. Wang, F. Zapata, G. Qian and E. B. Lobkovsky, *J. Am. Chem. Soc.*, 2008, **130**, 6718–6719; (e) Y. Cui, H. Xu, Y. Yue, Z. Guo, J. Yu, Z. Chen, J. Gao, Y. Yang, G. Qian and B. Chen, *J. Am. Chem. Soc.*, 2012, **134**, 3979–3982; (f) B. Chen, S. Xiang and G. Qian, *Acc. Chem. Res.*, 2010, **43**, 1115–1124; (g) Y.-Q. Lan, H.-L. Jiang, S.-L. Li and Q. Xu, *Adv. Mater.*, 2011, **23**, 5015–5020; (h) X.-Z. Song, S.-Y. Song, S.-N. Zhao, Z.-M. Hao, M. Zhu, X. Meng, L.-L. Wu and H.-J. Zhang, *Adv. Funct. Mater.*, 2014, **24**, 4034–4041; (i) Y. Takashima, V. M. Martínez, S. Furukawa, M. Kondo, S. Shimomura, H. Uehara, M. Nakahama, K. Sugimoto and S. Kitagawa, *Nat. Commun.*, 2011, **2**, 168–176; (j) X.-L. Yang, C. Zou, Y. He, M. Zhao, B. Chen, S. Xiang, M. O'Keeffe and C.-D. Wu, *Chem. - Eur. J.*, 2014, **20**, 1447–1452; (k) L.-Y. Zhang, J.-P. Zhang, Y.-Y. Lin and X.-M. Chen, *Cryst. Growth Des.*, 2006, **6**, 1684–1689; (l) S.-L. Zheng, J.-M. Yang, X.-L. Yu, X.-M. Chen and W.-T. Wong, *Inorg. Chem.*, 2004, **43**, 830.
- (a) P. Wu, J. Wang, C. He, X. Zhang, Y. Wang, T. Liu and C. Duan, *Adv. Funct. Mater.*, 2012, **22**, 1698–1703; (b) X. Zhao, X. Bu, T. Wu, S.-T. Zheng, L. Wang and P. Feng, *Nat. Commun.*, 2013, **4**, 2344; (c) D. Ma, B. Li, X. Zhou, Q. Zhou, K. Liu, G. Zeng, G. Li, Z. Shi and S. Feng, *Chem. Commun.*, 2013, **49**, 8964–8966; (d) Q.-K. Liu, J.-P. Ma and

- Y.-B. Dong, *J. Am. Chem. Soc.*, 2010, **132**, 7005–7017; (e) H.-L. Jiang, Y. Tatsu, Z.-H. Lu and Q. Xu, *J. Am. Chem. Soc.*, 2010, **132**, 5586–5587; (f) G.-L. Liu, Y.-j. Qin, L. Jing, G.-y. Wei and H. Li, *Chem. Commun.*, 2013, **49**, 1699–1701; (g) T. Wen, D.-X. Zhang, J. Liu, R. Lin and J. Zhang, *Chem. Commun.*, 2013, **49**, 5660–5662.
- 8 (a) J. Ferrando-Soria, P. Serra-Crespo, M. de Lange, J. Gascon, F. Kapteijn, M. Julve, J. Cano, F. Lloret, J. Pasán, C. Ruiz-Pérez, Y. Journaux and E. Pardo, *J. Am. Chem. Soc.*, 2012, **134**, 15301–15304; (b) Y.-N. Gong, L. Jiang, T.-B. Lu, J.-X. Ma, X.-F. Huang, X.-Q. Song and W.-S. Liu, *Chem. - Eur. J.*, 2013, **19**, 3590–3595; (c) X. Wang, X. Wang, Y. Wang and Z. Guo, *Chem. Commun.*, 2011, **47**, 8127–8129; (d) Q.-K. Liu, J.-P. Ma and Y.-B. Dong, *Chem. - Eur. J.*, 2009, **15**, 10364–10368; (e) Z. Chen, Y. Sun, L. Zhang, D. Sun, F. Liu, Q. Meng, R. Wang and D. Sun, *Chem. Commun.*, 2013, **49**, 11557–11559; (f) H. Li, W. Shi, K. Zhao, Z. Niu, H. Li and P. Cheng, *Chem. - Eur. J.*, 2013, **19**, 3358–3365; (g) R. Saha, B. Joarder, A. S. Roy, S. M. Islam and S. Kumar, *Chem. - Eur. J.*, 2013, **19**, 16607–16614; (h) W. J. Rieter, K. M. L. Taylor and W. Lin, *J. Am. Chem. Soc.*, 2007, **129**, 9852–9853; (i) N. B. Shustova, A. F. Cozzolino, S. Reineke, M. Baldo and M. Dincă, *J. Am. Chem. Soc.*, 2013, **135**, 13326–13329.
- 9 (a) Y.-S. Xue, Y. He, L. Zhou, F.-J. Chen, Y. Xu, H.-B. Du, X.-Z. You and B. Chen, *J. Mater. Chem. A*, 2013, **1**, 4525–4530; (b) H. Xu, F. Liu, Y. Cui, B. Chen and G. Qian, *Chem. Commun.*, 2011, **47**, 3153–3155; (c) A. Lan, K. Li, H. Wu, D. H. Olson, T. J. Emge, W. Ki, M. Hong and J. Li, *Angew. Chem., Int. Ed.*, 2009, **48**, 2334–2338; (d) S. Zhang, L. Han, L. Li, J. Cheng, D. Yuan and J. Luo, *Cryst. Growth Des.*, 2013, **13**, 5466–5472; (e) S. Pramanik, Z. Hu, X. Zhang, C. Zheng, S. Kelly and J. Li, *Chem. - Eur. J.*, 2013, **19**, 15964–15971; (f) S. Pramanik, C. Zheng, X. Zhang, T. J. Emge and J. Li, *J. Am. Chem. Soc.*, 2011, **133**, 4153–4155.
- 10 (a) Y. Li, S. Zhang and D. Song, *Angew. Chem., Int. Ed.*, 2013, **52**, 710–713; (b) J. Chen, F.-Y. Yi, H. Yu, S. Jiao, G. Pang and Z.-M. Sun, *Chem. Commun.*, 2014, **50**, 10506–10509.
- 11 (a) J.-M. Zhou, W. Shi, H.-M. Li, H. Li and P. Cheng, *J. Phys. Chem. C*, 2014, **118**, 416–426; (b) A. Planchais, S. Devautour-Vinot, S. Giret, F. Salles, P. Trens, A. Fateeva, T. Devic, P. Yot, C. Serre, N. Ramsahye and G. Maurin, *J. Phys. Chem. C*, 2013, **117**, 19393–19401.
- 12 (a) F.-Y. Yi, W. Yang and Z.-M. Sun, *J. Mater. Chem.*, 2012, **22**, 23201–23209; (b) P. Lama, R. Kumar Das, V. J. Smith and L. J. Barbour, *Chem. Commun.*, 2014, **50**, 6464–6467.
- 13 (a) V. A. Blatov, *Struct. Chem.*, 2012, **23**, 955–963. TOPOS software is available for download at <http://www.topos.samsu.ru>; (b) V. A. Blatov, *TOPOS, a Multipurpose Crystallochemical Analysis with the Program Package*, Russia, 2004; (c) M. O’Keeffe, Reticular Chemistry Structure Resource, <http://rcsr.anu.edu.au/>; (d) V. A. Blatov, A. P. Shevchenko and D. M. Proserpio, *Cryst. Growth Des.*, 2014, **14**, 3576–3586.
- 14 (a) A. L. Spek, *Acta Crystallogr., Sect. A: Found. Crystallogr.*, 1990, **46**, 194–201; (b) A. L. Spek, *PLATON99, a Multipurpose Crystallographic Tool*, Utrecht University, Utrecht, The Netherlands, 1999.
- 15 (a) C. A. Bauer, T. V. Timofeeva, T. B. Settersten, B. D. Patterson, V. H. Liu, B. A. Simmons and M. D. Allendorf, *J. Am. Chem. Soc.*, 2007, **129**, 7136–7144; (b) X.-L. Qi, R.-B. Lin, Q. Chen, J.-B. Lin, J.-P. Zhang and X.-M. Chen, *Chem. Sci.*, 2011, **2**, 2214–2218; (c) D. Yan, G. O. Lloyd, A. Delori, W. Jones and X. Duan, *ChemPlusChem*, 2012, **77**, 1112–1118; (d) D. Yan, Y. Tang, H. Lin and D. Wang, *Sci. Rep.*, 2014, **4**, 4337–4344; (e) Y. Tang, W. He, Y. Lu, J. Fielden, X. Xiang and D. Yan, *J. Phys. Chem. C*, 2014, **118**, 25365–25373; (f) D. Yan and D. G. Evans, *Mater. Horiz.*, 2014, **1**, 46–57.
- 16 (a) S. W. Thomas, G. D. Joly and T. M. Swager, *Chem. Rev.*, 2007, **107**, 1339–1386; (b) M. Zhang, G. Feng, Z. Song, Y.-P. Zhou, H.-Y. Chao, D. Yuan, T. T. Y. Tan, Z. Guo, Z. Hu, B. Z. Tang, B. Liu and D. Zhao, *J. Am. Chem. Soc.*, 2014, **136**, 7241–7244; (c) S. Dang, X. Min, W. Yang, F.-Y. Yi, H. You and Z.-M. Sun, *Chem. - Eur. J.*, 2013, **19**, 17172–17179.